

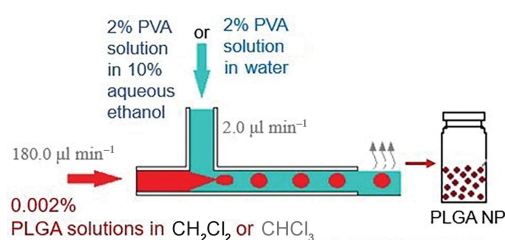
Easy size control of polymer nanoparticles obtained by emulsification–evaporation technique in a microfluidic reactor

Maria A. Merkulova,* Nadezhda S. Osipova, Olga O. Maksimenko,
Maria G. Gordienko and Svetlana E. Gelperina

*D. I. Mendeleev University of Chemical Technology of Russia, 125047 Moscow, Russian Federation.
Fax: +7 985 110 2033; e-mail: ma.merk@mail.ru*

DOI: 10.1016/j.mencom.2021.11.044

The production of polymer nanoparticles with a narrow size distribution on standard T- and X-configuration microfluidic chips with a channel size of 100 μm has been achieved. Introducing ethanol into the aqueous phase in 1 : 9 ratio (v/v) allowed one to reduce the surface tension of the contacting phases and obtain nanoparticles in the range of 100–150 nm. This makes our approach promising for development of nanoscale drug delivery systems.



Keywords: microfluidics, interfacial tension, emulsification–evaporation method, poly(lactide-*co*-glycolide) nanoparticles, drug delivery systems.

Nanoscale drug delivery systems are innovative dosage forms with a number of advantages.¹ Synthetic polymers are of particular interest as a carrier material, that provide high product reproducibility due to batch-to-batch uniformity, which makes it possible to predict drug loading and release rates from nanocarriers.^{2–4} Among them, FDA-approved polylactides (PLA) and copolymers of lactic and glycolic acid (PLGA) are widely used in pharmaceutical technology, particularly, for sustained-release formulations of various drug substances (Risplept Consta[®], Sandostatin LAR[®], *etc.*). One of the classical methods of polymer nanoparticles (PNPs) fabrication is emulsification of organic solutions of the polymers in aqueous phase followed by removal of the organic solvent.^{5–8} This process is divided into three stages: emulsion formation, removal of the organic solvent, and washing of the nanoparticles from unreacted components. The formation of an emulsion is the most important and difficult to control stage, since it is characterized by low reproducibility from batch to batch and wide size distribution of the obtained nanoparticles, thereby preventing the drug product from entering the market.⁹ The main tasks are to find the optimal dispersion mode in a turbulent flow (using various types of high-energy homogenizers) and to restrict the mass transfer caused by the premature removal of volatile organic solvents (such as chloroform, dichloromethane and ethyl acetate) used in the emulsion to dissolve the polymer and encapsulated substance. Microfluidic technologies have several advantages over the bulk methods, allowing controllable generation of monodisperse emulsion droplets without contact with the environment under homogeneous conditions. Forming droplets inside the microchip reduces the risks of disrupting the emulsification process due to the premature removal of the solvent from the system. In addition, the absence of turbulent flows of contacting phases in the chip guarantees high reproducibility of the formation of droplets of a given size. High scalability is an advantage of microfluidic technologies, however

necessity of individual designs of chips for various tasks leads to high costs. The width of the inner channel of standard mixing microchips restricts their use only to microparticles production.

Adjusting the ratio of the phases flow rates in the microfluidic chip makes it possible to control the size of the emulsion droplets; however, the minimal droplet size is determined by the interfacial tension forces and the capillary number, which is defined as:

$$Ca_{cr} = (\gamma\mu_c d_{max})/\sigma,$$

where Ca_{cr} is the critical capillary number, μ_c is the dynamic viscosity of the continuous phase, γ is the average velocity of the continuous phase, d_{max} is the maximum possible droplet size, σ is the interfacial tension between the continuous and dispersed phases (aqueous and organic, respectively). Based on this equation, the droplet size in any homogeneous system with a laminar flow can be controlled by varying the temperature of the contacting phases (*i.e.*, changing the dynamic viscosity), or adjusting the ratio of the phases flow rates, or changing the interfacial tension. Controlling the interfacial tension provides an energy-efficient approach to optimizing the formation of emulsion droplets that are small enough to form nanoparticles.

It was found that the size of the emulsion droplets could be reduced by introducing the cosolvent (*e.g.*, ethanol) miscible with the organic phase and water. The interfacial tension decreases by $\sim 2\text{--}2.5 \text{ mN m}^{-1}$ with the increase of ethanol concentration by every 6.25% (v/v), which results in the formation of smaller microparticles.⁹ This approach allows one to reduce the loading concentration of hydrophobic active pharmaceutical ingredients, because ethanol promotes rapid extraction of organic phase solvents into the external aqueous phase.

In this work, we for the first time explored the possibility of obtaining polymer nanoparticles of small size (100–300 nm) in a laminar flow of a microfluidic system using a standard 100 μm chip by introducing a non-toxic cosolvent ethanol into the aqueous phase.

Nanoparticles were prepared by emulsification followed by solvent evaporation using a Dolomite Microfluidics (UK) system equipped with two high-precision pressure driven P-pumps (Mitos Pressure pumps) coupled with two in-line Mitos Flow Rate Sensor controllers. Two chips of different flow geometry were used: T-shaped and X-shaped The Large Droplet Junction Chip. The internal channels of all chips are 100 μm wide and possesses a hydrophilic surface. Chips of both types were used for microparticles preparation (Online Supplementary Materials, Figure S1).

Resomer[®] RG 502H (Evonik Röhm GmbH, Germany), a low molecular weight PLGA (50 : 50, acid terminated, M_w 7,000–17,000 Da) was chosen as the carrier polymer. It is one of the commonly used types for nanoparticles preparation, which provides fast drug release to target organs.^{6,10} To dissolve the polymer, we used immiscible with water organic solvents, chloroform and dichloromethane.

To prevent agglomeration or coalescence of emulsion droplets, steric stabilizers has been introduced into the aqueous phase. We chose polyvinyl alcohol (PVA, 9–10 kDa, 80% hydrolysed), which is frequently used in the preparation of PLGA NPs in concentrations from 0.5 to 2.0% (w/v).¹¹ To select the optimal concentrations of the stabilizer (PVA and PVA with addition of EtOH), the critical micelle concentration (CMC) was determined by measuring the surface tension. The surface tension *versus* time was measured at the organic–aqueous interface.[†] The CMC of the aqueous PVA solution was achieved at the concentration of 2.1 mM [Figure 1(a)], hence, further increase in the PVA concentration was inappropriate. Changing the composition of the aqueous phase by adding EtOH to a 2% PVA solution [Figure 1(b)] further reduces the surface tension of the aqueous phase, thus, the surface tension value decreased from 47.6 to 46.7 mN m^{-1} when using 10% EtOH (v/v). A further increase in the concentration of EtOH in a 2% aqueous solution of PVA did not cause any significant changes of surface tension.

The organic phase was a solution of PLGA in CHCl_3 or CH_2Cl_2 (2 mg ml^{-1}), and the aqueous phase was 2% PVA solution in water or in 10% (w/v) EtOH. Solutions were preliminarily filtered through 0.2- μm filter and degassed, then injected into the chip at different flow rates: 2, 3, 5 $\mu\text{l min}^{-1}$ for

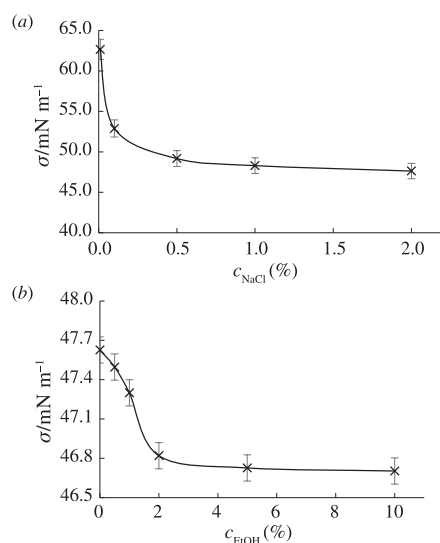


Figure 1 Effect of the aqueous phase composition on the surface tension: (a) aqueous solutions of PVA; (b) 2% aqueous solutions of PVA with the addition of EtOH (9 : 1, v/v).

[†] The measurements of the interfacial tension at the interface between the phases of the emulsion were carried out using a dynamic pendant drop method with a drop tensiometer (Tracker[®], France).

Table 1 Comparison of the size parameters of the obtained PLGA nanoparticles, depending on the composition of the aqueous (AP) and organic (OP) phases using T- or X-type chips ($n = 3$).^a

| Phase composition | | Chip type | Flow rate/ $\mu\text{l min}^{-1}$ | | Mean size and size distribution | | | |
|--|------------------------------|-----------|--------------------------------------|-------|---------------------------------|------|------|------|
| OP | AP | | OP | AP | d_{av}/nm | SD | PDI | SD |
| 0.02% PLGA in CH_2Cl_2 | 2% PVA in water | T | 2.0 | 180.0 | 352.4 | 55.5 | 0.30 | 0.10 |
| | | X | 3.0 | 200.0 | 338.4 | 64.5 | 0.25 | 0.04 |
| 0.02% PLGA in CHCl_3 | 2% PVA in water–EtOH (9 : 1) | T | 2.0 | 180.0 | 100.5 | 6.6 | 0.08 | 0.02 |
| | | X | 3.0 | 200.0 | 102.4 | 14.4 | 0.08 | 0.03 |
| 0.02% PLGA in CHCl_3 | 2% PVA in water | T | 2.0 | 180.0 | 621.3 | 61.2 | 0.25 | 0.25 |
| | | X | 3.0 | 200.0 | 500.0 | 22.4 | 0.33 | 0.10 |
| 0.02% PLGA in CHCl_3 | 2% PVA in water–EtOH (9 : 1) | T | 2.0 | 180.0 | 292.3 | 12.4 | 0.28 | 0.10 |
| | | X | 3.0 | 200.0 | 271.2 | 9.8 | 0.22 | 0.03 |

^a SD is the standard deviation; d_{av} is the average size (hydrodynamic diameter), and PDI is the polydispersity index.

organic phase and 100, 125, 150, 180, 200 and 225 $\mu\text{l min}^{-1}$ for aqueous phase. The emulsion droplets formed inside the chip were collected in a vial filled with water under constant stirring (500 rpm), and the residual organic solvent was removed *in vacuo* on a rotary evaporator (25–40 $^{\circ}\text{C}$, 20 mbar).

In the case of using CHCl_3 , PLGA NPs had a larger size (270–620 nm) and a wide PDI (>0.2), regardless of the phase composition or the ratio of the flow rates (Table 1).[‡] This can be explained by the conformation of the polymer chain in the solvent under the influence of opposing forces: the interaction between the segments of the polymer chain, which leads to the folding of the macromolecule into a tangle, and interactions between the segments of the chain and solvent molecules, which repel the segments, causing the loosening of the tangle.

As a result of these interactions, the volume of the polymer coil can increase owing to the penetration of solvent molecules into it. This leads to the limitation of mobility in solution and to the increase in intermolecular friction.¹² Thus, viscosity is a measure of the hydrodynamic volume of a polymer coil: in a ‘good’ solvent the macromolecular coil swells, and the polymer solution is more viscous than the solution in a ‘bad’ solvent. This hypothesis was confirmed by determining the viscosity of PLGA solutions in CH_2Cl_2 and CHCl_3 [§] *via* measuring the flow time of polymer solutions of different concentrations (1.56–50 mg ml^{-1}) compared with pure solvent at 20 $^{\circ}\text{C}$ (Figure 2).

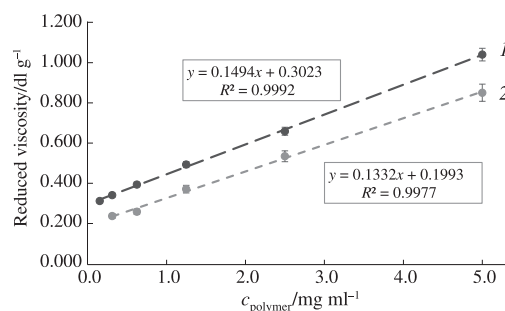


Figure 2 Reduced viscosity vs. polymer concentration of PLGA solutions in (1) CHCl_3 and (2) CH_2Cl_2 .

[‡] The NPs size and polydispersity index (PDI) were determined by dynamic light scattering using a Zetasizer Nano ZS (Malvern, UK).

[§] The viscosity of PLGA solutions in organic solvents was determined on a capillary viscometer (VPZh-4, OOO EKROSKHIM, Russia) with a glass capillary (inner diameter 0.37 mm).

Table 2 Physicochemical characteristics of PLGA solutions in organic solvents at 20 °C.^a

| Solvent | $\rho/\text{g cm}^{-3}$ | $[\eta]/\text{dl g}^{-1}$ | K_H |
|---------------------------------|-------------------------|---------------------------|--------------|
| CH ₂ Cl ₂ | 1.33 | 0.199 ± 0.01 | 3.353 ± 0.01 |
| CHCl ₃ | 1.49 | 0.302 ± 0.01 | 1.638 ± 0.01 |

^a ρ is density, $[\eta]$ is intrinsic viscosity, K_H is the Huggins constant.

Standard methods were used to calculate relative (η_{rel}), specific (η_{sp}) and reduced (η_{red}) viscosities. The intrinsic viscosity $[\eta]$ of the solutions was determined by extrapolating the values of the reduced viscosity (η_{red}) to zero concentration. We also calculated the Huggins constant K_H ,¹³ which characterizes the interaction of macromolecules in a solvent, as:

$$\eta_{\text{red}} = \eta_{\text{sp}}/c = [\eta] + K_H[\eta]^2c,$$

where c is the concentration of the solution. The intrinsic viscosity of PLGA solution in CHCl₃ is higher than in CH₂Cl₂ (Table 2). K_H is smaller in CHCl₃, which indicates the higher affinity of the solvent for the polymer. The results correlate with previously published data.¹⁴

Then we studied interfacial tension in the polymer–organic solvent–aqueous phase system. The organic phase was a PLGA solution in CH₂Cl₂ or CHCl₃ in different concentrations, the aqueous phase contained 2% PVA in water or in 10% ethanol (Figure 3). To create the stable nanoscale emulsion droplets, even a slight decrease in the interfacial tension can be crucial. It has been shown that the use of ethanol reduces interfacial tension in both systems, regardless of the polymer concentration, as follows: from 2.65 to 1.9 mN m⁻¹ for PLGA–CHCl₃–PVA system [see Figure 3(a)] and from 3.4 to 2.4 mN m⁻¹ for PLGA–CH₂Cl₂–PVA system [see Figure 3(b)]. This leads to the reduction of PLGA NPs size by more than half for both types of solvents and to the narrow size distribution (see Table 1). This is explained by the Marangoni effect associated with a decrease in the interfacial tension in the system.¹⁵

Polymer nanoparticles obtained when using CH₂Cl₂ and 10% EtOH in 2% aqueous PVA solution possess the smallest size (100.5–102.4 nm) and are characterized by a narrow distribution,

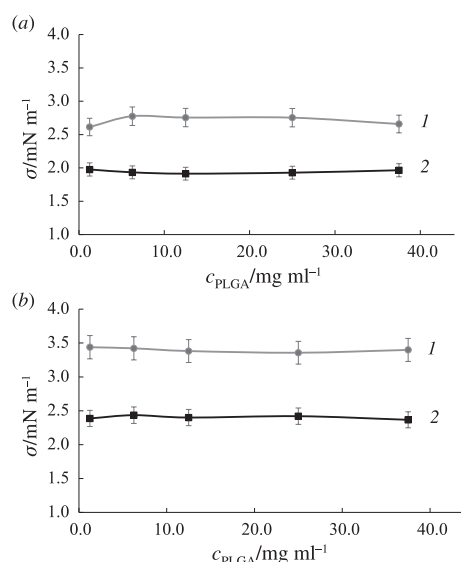


Figure 3 Interfacial tension at different PLGA concentrations: (a) PLGA solution in CH₂Cl₂ and 2% PVA solution in (1) water and (2) 10% EtOH; (b) PLGA solution in CHCl₃ and 2% PVA solution in (1) water and (2) 10% EtOH.

† TEM PLGA NPs images were obtained using a Tecnai™ 12 G2 BioTwin Spirit transmission electron microscope with an Eagle 4K detector, ThermoFisher Scientific; accelerating voltage 120 kV, contrast agent – 1% uranyl acetate.

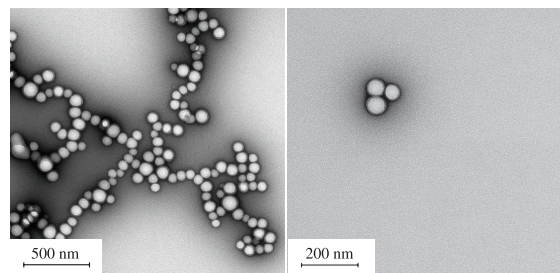


Figure 4 TEM images of PLGA NPs prepared on X-type microfluidic chip using CH₂Cl₂ and 10% EtOH in 2% aqueous PVA solution.

which is confirmed by the low PDI value (<0.1) and transmission electronic microscopy data (Figure 4).[†]

This size of nanoscale delivery systems is optimal for intravenous administration and passive delivery to the tumor owing to the effect of increased permeability and retention (EPR effect).¹⁶ The data obtained allows one to expand the use of designed mixing chips to obtain microparticles, that might reduce the costs of the production.¹⁷

In conclusion, changing the composition of the aqueous phase by adding a cosolvent makes it possible to control the size and polydispersity of PLGA nanoparticles produced *via* emulsification followed by the solvent removal. The size range of obtained nanoparticles (100–150 nm) is of particular interest for creating the nanoscale drug delivery systems.

This work was carried out with the financial support of the Russian Foundation for Basic Research within the framework of scientific project no. 20-015-00381/20.

Online Supplementary Materials

Supplementary data associated with this article can be found in the online version at doi: 10.1016/j.mencom.2021.11.044.

References

- 1 T. Tagami and T. Ozeki, *J. Pharm. Sci. (Philadelphia, PA, U. S.)*, 2017, **106**, 2219.
- 2 S. Gibaud, M. Demoy, J. P. Andreux, C. Weingarten, B. Gouritin and P. Couvreur, *J. Pharm. Sci.*, 1996, **85**, 944.
- 3 J. M. Lee, B.-C. Lee and S.-J. Hwang, *J. Chem. Eng. Data*, 2000, **45**, 1162.
- 4 M. S. Oshchepkov, A. S. Semyonkin, A. O. Menkov, P. A. Melnikov, M. P. Valikhov, I. N. Solovieva, S. V. Tkachenko and J. A. Malinowskaya, *Mendeleev Commun.*, 2020, **30**, 747.
- 5 F. Y. Han, K. J. Thurecht, A. K. Whittaker and M. T. Smith, *Front. Pharmacol.*, 2016, **7**, 185.
- 6 C. Fornaguera, N. Feiner-Gracia, G. Calderó, M. J. García-Celma and C. Solans, *Nanoscale*, 2015, **7**, 12076.
- 7 D. Liu, H. Zhang, F. Fontana, J. T. Hirvonen and H. A. Santos, *Lab Chip*, 2017, **17**, 1856.
- 8 X. Li and X. Jiang, *Adv. Drug Delivery Rev.*, 2018, **128**, 101.
- 9 H. Ragelle, F. Danhier, V. Préat, R. Langer and D. G. Anderson, *Expert Opin. Drug Delivery*, 2017, **14**, 851.
- 10 S. Sharma, A. Parmar, S. Kori and R. Sandhir, *TrAC, Trends Anal. Chem.*, 2016, **80**, 30.
- 11 Yu. V. Chernysheva, V. G. Babak, N. R. Kildeeva, F. Boury, J. P. Benoit, N. Ubrich and P. Maincent, *Mendeleev Commun.*, 2003, **13**, 65.
- 12 C. E. Astete and C. M. Sabliov, *J. Biomater. Sci., Polym. Ed.*, 2006, **17**, 247.
- 13 I. V. Shulyak and E. I. Grushova, *Trudy BGTU. Seriya IV (Proceedings of BSTU. Series IV). Khimiya, tekhnologiya organicheskikh veshchestv i biotekhnologiya*, 2009, 92 (in Russian).
- 14 C. I. C. Crucho and M. T. Barros, *Mater. Sci. Eng., C*, 2017, **80**, 771.
- 15 I. U. Khan, C. A. Serra, N. Anton and T. Vandamme, *J. Control. Release*, 2013, **172**, 1065.
- 16 R. Saka and N. Chella, *Environ. Chem. Lett.*, 2021, **19**, 1097.
- 17 A. G. Niculescu, C. Chircov, A. C. Bîrcă and A. M. Grumezescu, *Int. J. Mol. Sci.*, 2021, **22**, 2011.

Received: 23rd March 2021; Com. 21/6504